CrossMark

GaInN light-emitting diodes using separate epitaxial growth for the p-type region to attain polarization-inverted electron-blocking layer, reduced electron leakage, and improved hole injection

David S. Meyaard,[1,a)] Guan-Bo Lin,[1] Ming Ma,[1] Jaehee Cho,[1,2] E. Fred Schubert,[1] Sang-Heon Han,[3] Min-Ho Kim,[3] HyunWook Shim,[3] and Young Sun Kim[3]
[1]*Future Chips Constellation, Department of Electrical, Computer, and Systems Engineering, Rensselaer Polytechnic Institute, Troy, New York 12180, USA*
[2]*Semiconductor Physics Research Center, School of Semiconductor and Chemical Engineering, Chonbuk National University, Jeonju 561-756, Korea*
[3]*LED Business, Samsung Electronics, Yongin 446-920, Korea*

(Received 8 August 2013; accepted 26 October 2013; published online 13 November 2013)

A GaInN light-emitting diode (LED) structure is analyzed that employs a separate epitaxial growth for the p-type region, i.e., the AlGaN electron-blocking layer (EBL) and p-type GaN cladding layer, followed by wafer or chip bonding. Such LED structure has a polarization-inverted EBL and allows for uncompromised epitaxial-growth optimization of the p-type region, i.e., without the need to consider degradation of the quantum-well active region during p-type region growth. Simulations show that such an LED structure reduces electron leakage, reduces the efficiency droop, improves hole injection, and has the potential to extend high efficiencies into the green spectral region. © *2013 AIP Publishing LLC*. [http://dx.doi.org/10.1063/1.4829576]

The efficiency droop has been identified as the single most significant loss mechanism in GaInN light-emitting diodes (LEDs).[1] The efficiency droop has a pronounced wavelength dependence with green devices (525 nm) suffering the most from the efficiency droop, blue devices (450 nm) suffering less than green devices, and violet devices (405 nm) suffering less than blue devices.[1] Considering the widespread deployment of GaInN LEDs in general lighting applications, an improvement in the efficiency by overcoming the efficiency droop would have substantial consequences. Likewise, extending high efficiencies to the green spectral region would fundamentally change the capabilities of LEDs by enabeling high efficiency devices across the entire visible spectrum.

Experimental investigations on the efficiency droop have revealed that the carrier-recombination-loss mechanism causing the efficiency droop has a strong 3rd order ($n_{QW}{}^3$) dependence and a weaker 4th order ($n_{QW}{}^4$) dependence, where n_{QW} is the free electron concentration in the quantum-well (QW).[2] Recombination of electron-hole pairs in a current-injected LED structure has been described by[2]

$$\begin{aligned} R &= A_{SRH}\, n_{QW} + B n_{QW}{}^2 + C_{Auger} n_{QW}{}^3 + \mathrm{f}(n_{QW}), \\ &= A_{SRH}\, n_{QW} + B n_{QW}{}^2 + C_{Auger} n_{QW}{}^3 \\ &\quad + C_{DL} n_{QW}{}^3 + D_{DL} n_{QW}{}^4, \end{aligned} \tag{1}$$

where $\mathrm{f}(n_{QW})$ describes the electron leakage out of the active region, C_{DL} and D_{DL} are the 3rd and 4th order drift-leakage coefficients, respectively,[2] and the other symbols have their usual meaning. Multiple models have been proposed to explain the efficiency droop,[3–10] two of which have been quantitatively refined and shown to have, consistent with experiments, a strong 3rd order dependence on n_{QW}: These two models are the electron-drift-leakage model,[2,9] and the Auger model.[7,8] Inspection of Eq. (1) shows that both models have a recombination term that has the generally accepted $n_{QW}{}^3$ dependence.

Within the framework of the electron-drift-leakage model, the 3rd-order drift-leakage coefficient, C_{DL}, given in Eq. (1), can be expressed as[2]

$$C_{DL} = \frac{n_{Barrier}}{n_{QW}} \frac{\mu_n}{\mu_p\, p_{p0}} B = \frac{\delta\, \mu_n}{\mu_p\, p_{p0}} B, \tag{2}$$

where δ is the ratio of the electron concentration in the barrier to the electron concentration in the QW of the active region, and p_{p0} is the hole concentration in the p-type layer. Using $\delta = 10^{-3}$, $p_{p0} = 5 \times 10^{17}\,\mathrm{cm^{-3}}$, $\mu_p = 5\ \mathrm{cm^2\ V^{-1}\ s^{-1}}$, $\mu_n = 250\ \mathrm{cm^2\ V^{-1}\ s^{-1}}$, and $B = 10^{-10}\ \mathrm{cm^3\ s^{-1}}$, we estimate the C_{DL} coefficient to be on the order of $10^{-29}\ \mathrm{cm^6\ s^{-1}}$, consistent with experimental reports. The equation shows that an improvement in the efficiency droop can be attained by reducing δ and enhancing p_{p0}. Next, we will show that the LED structure presented here reduces C_{DL} (and thus the efficiency droop) by reducing δ and by enhancing p_{p0}. It has been shown that a high acceptor concentration at the QW/spacer/electron-blocking layer (EBL) interface is vital to reduce electron leakage.[11]

Conventional GaInN LED epitaxial layers are grown in a single epitaxial growth run. We propose an alternative strategy in which the LED epitaxial layers are grown in two separate growth runs. The proposed method of LED growth is schematically shown in Figure 1. The first growth run provides a buffer layer, the n-type GaN cladding layer, and the multi-quantum well (MQW) active region, fully optimized for efficient light-emission. The first epitaxial-layer stack concludes with the growth of a thin GaN spacer layer to protect the GaInN QWs and provide a layer suitable for wafer-bonding. The second growth run provides the p-type portion

a)Electronic mail: meyaad@rpi.edu

© 2013 AIP Publishing LLC

This article is copyrighted as indicated in the abstract. Reuse of AIP content is subject to the terms at: http://scitation.aip.org/termsconditions. Downloaded to IP: 128.113.121.12 On: Wed, 13 Nov 2013 16:50:12

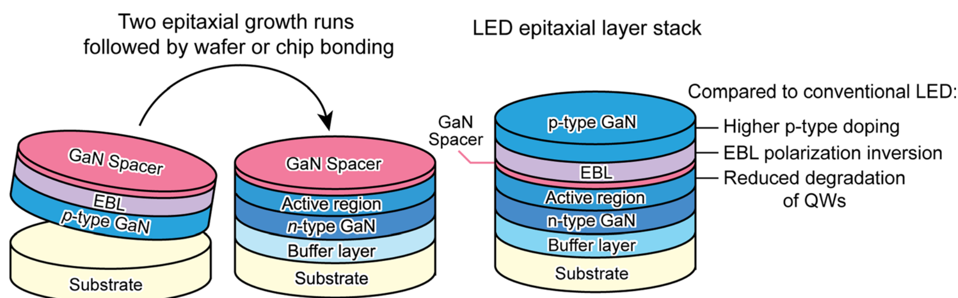

FIG. 1. Schematic of growth and fabrication of GaInN LED with a separately grown p-type GaN to attain a polarization-inverted EBL and enhanced hole-transport properties.

of the LED, that is, the top p-type GaN cladding layer, the EBL, and a thin GaN spacer layer suitable for wafer-bonding. Subsequently, the two partial LED structures are combined via a wafer or chip bonding process to form a single wafer (or chip) with the full LED structure. The spacer layer is a critical layer since it serves as the interface of the wafer/chip bonding process. A concern is that the spacer layer may be consumed or damaged during the wafer/chip bonding process. However, it is well established that the c-plane of GaN, (top surface, {0001}, Ga face), is impervious to wet chemical etching. Given this unique and advantageous property, even a very thin spacer layer could be very suitable for the wafer/chip bonding process. Subsequent to the wafer/chip bonding process, the sapphire substrate of the p-type epitaxial layer may be removed by using a substrate-removal process such as laser lift-off (LLO), in order to make accessible the p-type GaN cladding layer. The resulting LED epitaxial wafer is now similar to a conventional LED epitaxial wafer, with the following exceptions: (i) the polarization charges in the EBL are reversed; (ii) the growth conditions of the p-type region (particularly the growth temperature) can be optimized without constraint; (iii) the MQW active region will not degrade during the p-type region growth. The substrate on the resulting epilayer stack may be removed if vertical-current flow LEDs are desired, or may be left attached if lateral-geometry LEDs are desired. As will be discussed next, such LED structure and process have several beneficial properties.

First, as a consequence of the two separate growths, the polarization charges in the EBL are inverted. Conventional GaInN LEDs have an electron-attracting positive polarization-sheet charge at the spacer-EBL interface. This sheet charge reduces the EBL barrier thereby enhancing electron leakage out of the active region.[3,4,10,12] However, the LED structure shown in Figure 1 has a negative polarization charge at the spacer-EBL interface which aids in the electron confinement to the active region.

Second, the LED process discussed here allows for uncompromised optimization of the p-type region. In conventional GaInN LEDs, the p-type GaN is grown *after* the QW active region, so that the p-type-layer growth temperature is limited to values that minimize the degradation of the QW active region. This limitation forces the growth temperature for the post-QW p-type region to be lower than optimal values, particularly for green-emitting LEDs. That is, the p-type region of green devices is grown at lower temperatures than that of violet devices; although this preserves the integrity of the QWs, it compromises the doping characteristics of the p-type region. That is, a compromise is forced between (i) maintaining the integrity of the QWs and (ii) optimizing the p-type layer growth. If optimized (higher) growth temperatures were possible, the hole concentration would be enhanced, thereby reducing carrier overflow.[2,9]

Third, the integrity of the MQW active region is not compromised by the growth of post-QW layers. High-temperature epitaxial growth of the post-QW layers degrades the MQW active region and reduces the efficiency of the LED. This is particularly relevant for green-emitting devices, whose active region is more sensitive to prolonged exposure to high temperatures. The proposed LED process eliminates the QWs' prolonged exposure to high temperatures that occurs in conventional GaInN LEDs, during the p-type layer growth.

To verify the advantages of the proposed LED structure, APSYS simulations are performed for a conventional LED and an LED based on the growth scheme presented above. This simulation software computes the wurtzite electron band structure of the strained quantum wells, self-consistently computes the carrier transport, and calculates the photon emission spectrum. The transport model includes drift and diffusion of electrons and holes, Fermi statistics, built-in polarization and thermionic emission at hetero-interfaces, as well as Shockley-Read-Hall and Auger recombination. Quantum transport models (such as tunneling) are not considered in the present simulation. The LEDs in the simulation have an active-region with three undoped 3 nm thick GaInN QWs and 4 nm undoped GaN quantum barriers (QBs). We have generally found that the parameters of the p-type region and active region are of primary and secondary importance, respectively, in determining the electron leakage out of the active region. We employ a 30 nm $Al_{0.15}Ga_{0.85}N$ EBL in the simulation. The conduction band offset ratio $\Delta E_C/\Delta E_g$ is assumed to be 0.6 for the AlGaN EBL, with an acceptor concentration of $2 \times 10^{18}\,cm^{-3}$ and an activation energy of 200 meV. The p-type GaN is doped with $1 \times 10^{19}\,cm^{-3}$ acceptors having an activation energy of 170 meV, which results in a free hole concentration in the low $10^{17}\,cm^{-3}$ range. An Auger coefficient of $10^{-32}\,cm^6/s$ is chosen for the simulation, consistent with theoretical expectation.[13] The polarization charge employed in this simulation is 50% of the theoretical Bernardini values.[14] Figure 2 shows the simulated band diagrams of the LED structures at a current density of 200 A/cm^2. Several key differences can be identified from this figure, which will be discussed next.

Conventional GaInN LEDs contain a positive polarization-sheet charge at the spacer-EBL interface. This sheet electron-attracting charge promotes electron leakage out of the active region. Comparing the spacer/EBL interface

This article is copyrighted as indicated in the abstract. Reuse of AIP content is subject to the terms at: http://scitation.aip.org/termsconditions. Downloaded to IP: 128.113.121.12 On: Wed, 13 Nov 2013 16:50:12

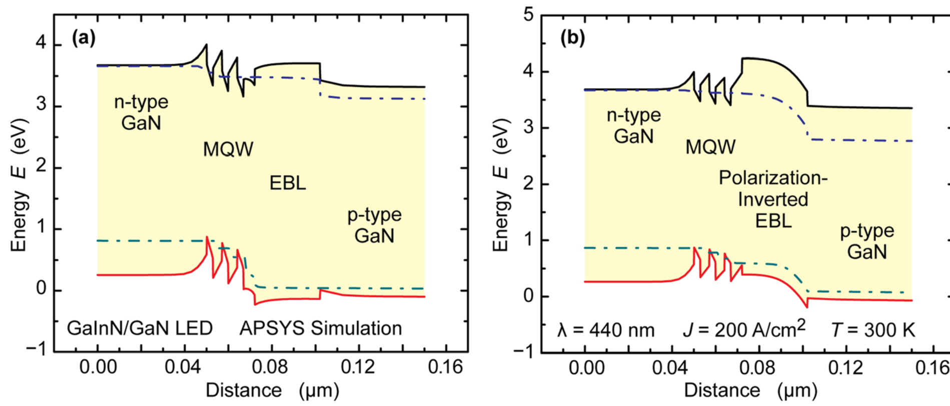

FIG. 2. Simulated band diagrams of (a) conventional GaInN LED and (b) LED with polarization inverted EBL, shown at 200 A/cm^2.

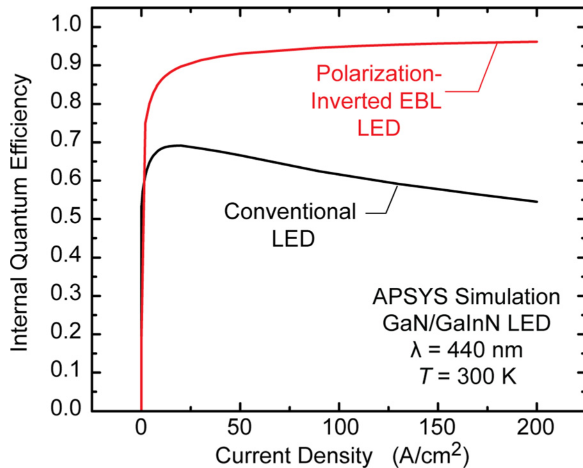

FIG. 3. Simulated internal quantum efficiency as a function of current density for a conventional LED and the LED with polarization-inverted EBL.

of Figs. 2(a) and 2(b), it is clear that the electrons are attracted to this interface in the conventional LED. In contrast to this, Fig. 2(b) shows an interface with the opposite, i.e., negative sheet charge, which repels electrons, thereby hindering their escape from the active region. The conduction-band energy difference from the bottom of the last quantum well to the top of the EBL is 0.44 eV for the conventional LED structure and 0.78 eV for the LED with polarization-inverted EBL. The difference between these two values is due to the inverted polarization charge at the spacer/EBL interface. Given a Boltzmann distribution of carriers in the quantum wells, this difference in barrier height for electrons leads to a stronger carrier confinement and thus reduced electron overflow. Furthermore, considering the conduction-band edge of a conventional LED, the energy of electrons located at the highest-energy point of any of the QBs of the MQW is higher than the highest-energy point of the EBL, as inferred from Fig. 2(a). This can increase the fraction of electrons that overshoot the QWs and escape from the active region (by means of quasi-ballistic transport).[10]

Our simulations demonstrate an advantageous effect of EBL-polarization inversion on the efficiency droop. Figure 3 shows the simulated internal quantum efficiency (IQE) of the conventional LED as well as the LED with polarization-inverted EBL. The conventional LED has peak IQE of approximately 70% at a current density of 20 A/cm^2. We note that simulation of an LED structure with no EBL results in a lower peak IQE and stronger droop. The LED with a polarization-inverted EBL shows no efficiency droop in this current range, with much higher efficiency. We attribute the efficiency gain to reduced electron leakage from the active region.

In order to illustrate the effect of reduced electron leakage at high currents, we study the electron concentration across the LED's layers at high current densities. Figure 4(a) shows the electron concentration as a function of position for the conventional LED and the LED with polarization-inverted EBL. Inspection of the figure reveals that the LED with polarization-inverted EBL shows lower electron concentration in the p-type GaN. Fig. 4(b) shows the local electron current density across the LED. At 200 A/cm^2, the conventional LED shows a significant electron current in the p-type region. In contrast to this, the LED with polarization inverted EBL shows negligible current in the p-type region. This reduction in electron leakage explains the improved efficiency droop properties shown in Fig. 3.

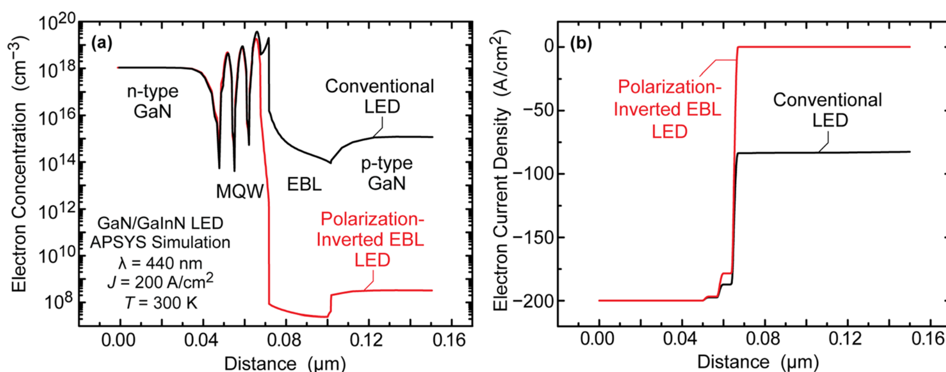

FIG. 4. (a) Simulated local electron concentration and (b) local electron current of conventional GaInN LED and LED with polarization inverted EBL, shown at 200 A/cm^2.

This article is copyrighted as indicated in the abstract. Reuse of AIP content is subject to the terms at: http://scitation.aip.org/termsconditions. Downloaded to IP: 128.113.121.12 On: Wed, 13 Nov 2013 16:50:12

We note that the other anticipated advantages of the new LED structure, i.e., (i) enhanced p-type doping and (ii) reduced degradation of the active region, as discussed above, are not included in the simulation. These two advantages should further improve the characteristics of the LED structure and process presented here.

A particular challenge in realizing such an EBL-polarization-inverted LED structure is the wafer- or chip-bonding process. This is because the realization of the LED structure presented here requires a wafer- or chip-bonding process that is (i) precise at the atomic level so that the continuity of the band structure is not disrupted across the bonding interface and (ii) does not require treatments at excessively high temperatures so that the integrity of the QW active region is preserved. Bonding processes such as metal-based[15,16] or adhesive-polymer-based processes[17,18] are not suitable for the current EBL-polarization-inverted LED structure. A potentially suitable bonding process is the semiconductor-to-semiconductor wafer-bonding process in which the adhesion is primarily seen as a result of van der Waals forces.[19] The direct-wafer-bonding process has already been implemented in III-V semiconductor material systems such as AlGaInP/GaP[20–22] and GaAs/InP,[23] and its application to GaN/GaN interfaces could enable the fabrication of the EBL-polarization-inverted LED structure. Given the anticipated advantages of the EBL-polarization-inverted LED, the availability of a GaN-to-GaN wafer-bonding process would be desirable.

In conclusion, we have presented a GaInN LED structure and process that significantly deviate from conventional GaInN LEDs in terms of implementation and properties. The LED structure, which requires a wafer- or chip-bonding process, has a polarization-inverted EBL with an electron-repelling negative polarization sheet charge at the spacer-EBL interface and allows for the uncompromised optimization of the p-type GaN layer without compromising the quality of the GaInN QWs of the active region. We show that this structure has the potential of extending high efficiencies to the green wavelength region which has long suffered from a severe efficiency droop. Simulations are performed for LED structures having an EBL with (i) conventional polarization and (ii) inverted polarization. The results show a strong reduction in efficiency droop and the associated C_{DL} coefficient.

The authors gratefully acknowledge support by Samsung Electronics Company and the Korean Ministry of Knowledge Economy and Korea Institute for Advancement of Technology (KIAT) through the International Collaborative R&D Program. Author J. Cho acknowledges support by the Basic Research Laboratory Program (No. 2011-0027956) and Priority Research Centers Program (No. 2009-0094031) through the National Research Foundation of Korea funded by the Ministry of Education, Science and Technology.

[1]J. Cho, E. F. Schubert, and J. K. Kim, Laser Photonics Rev. **7**, 408 (2013).
[2]G.-B. Lin, D. Meyaard, J. Cho, E. F. Schubert, H. Shim, and C. Sone, Appl. Phys. Lett. **100**, 161106 (2012).
[3]M.-H. Kim, M. F. Schubert, Q. Dai, J. K. Kim, E. F. Schubert, J. Piprek, and Y. Park, Appl. Phys. Lett. **91**, 183507 (2007).
[4]I. V. Rozhansky and D. A. Zakheim, Semiconductors **40**, 839 (2006).
[5]T. Mukai, M. Yamada, and S. Nakamura, Jpn. J. Appl. Phys., Part 1 **38**, 3976 (1999).
[6]Y. Yang, X. A. Cao, and C. Yan, IEEE Trans. Electron Devices **55**, 1771 (2008).
[7]Y. C. Shen, G. O. Mueller, S. Watanabe, N. F. Gardner, A. Munkholm, and M. R. Krames, Appl. Phys. Lett. **91**, 141101 (2007).
[8]F. Bertazzi, M. Goano, and E. Bellotti, Appl. Phys. Lett. **101**, 011111 (2012).
[9]D. S. Meyaard, G.-B. Lin, Q. Shan, J. Cho, E. F. Schubert, H. Shim, M.-H. Kim, and C. Sone, Appl. Phys. Lett. **99**, 251115 (2011).
[10]M. F. Schubert and E. F. Schubert, Appl. Phys. Lett. **96**, 131102 (2010).
[11]J. Piprek and S. Li, Opt. Quantum Electron. **42**, 89 (2010).
[12]M. F. Schubert, J. Xu, J.-K. Kim, E. F. Schubert, M.-H. Kim, S. Yoon, S. M. Lee, C. Sone, T. Sakong, and Y. Park, Appl. Phys. Lett. **93**, 041102 (2008).
[13]F. Bertazzi, M. Goano, and E. Bellotti, Appl. Phys. Lett. **97**, 231118 (2010).
[14]F. Bernardini, in *Nitride Semiconductor Devices: Principles and Simulation*, edited by J. Piprek (Wiley-VCH, Weinheim, 2007), pp. 49–67.
[15]T.-I. Kim, Y. H. Jung, J. Song, D. Kim, Y. Li, H.-S. Kim, I.-S. Song, J. J. Wierer, H. A. Pao, Y. Huang, and J. A. Rogers, Small **8**, 1643 (2012).
[16]W. S. Wong, T. Sands, N. W. Cheung, M. Kneissl, D. P. Bour, P. Mei, L. T. Romano, and N. M. Johnson, Appl. Phys. Lett. **77**, 2822 (2000).
[17]Y. J. Lee, P. C. Lin, T. C. Lu, H. C. Kuo, and S. C. Wang, Appl. Phys. Lett. **90**, 161115 (2007).
[18]G. Roelkens, J. Van Campenhout, J. Brouckaert, D. Van Thourhout, R. Baets, P. Rojo Romeo, P. Regreny, A. Kazmierczak, C. Seassal, X. Letartre, G. Hollinger, J. M. Fedeli, L. Di Cioccio, and C. Lagahe-Blanchard, Mater. Today **10**, 36 (2007).
[19]A. Plößl and G. Kräuter, Materials Science and Engineering: R: Reports **25**(1), 1 (1999).
[20]G. E. Höfler, D. A. Vanderwater, D. C. DeFevere, F. A. Kish, M. D. Camras, F. M. Steranka, and I.-H. Tan, Appl. Phys. Lett. **69**, 803 (1996).
[21]F. A. Kish, D. A. Vanderwater, M. J. Peanasky, M. J. Ludowise, S. G. Hummel, and S. J. Rosner, Appl. Phys. Lett. **67**, 2060 (1995).
[22]F. A. Kish, F. M. Steranka, D. C. DeFevere, D. A. Vanderwater, K. G. Park, C. P. Kuo, T. D. Osentowski, M. J. Peanasky, J. G. Yu, R. M. Fletcher, D. A. Steigerwald, M. G. Craford, and V. M. Robbins, Appl. Phys. Lett. **64**, 2839 (1994).
[23]Z. L. Liau and D. E. Mull, Appl. Phys. Lett. **56**, 737 (1990).

This article is copyrighted as indicated in the abstract. Reuse of AIP content is subject to the terms at: http://scitation.aip.org/termsconditions. Downloaded to IP: 128.113.121.12 On: Wed, 13 Nov 2013 16:50:12